



Contents lists available at ScienceDirect

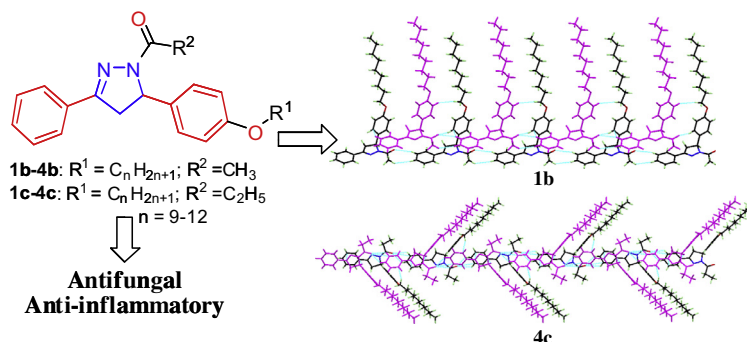
## Spectrochimica Acta Part A: Molecular and Biomolecular Spectroscopy

journal homepage: [www.elsevier.com/locate/saa](http://www.elsevier.com/locate/saa)Synthesis, spectral characterization, self-assembly and biological studies of *N*-acyl-2-pyrazolines bearing long alkoxy side chainsAsghar Abbas<sup>a,\*</sup>, Habiba Nazir<sup>b</sup>, Muhammad Moazzam Naseer<sup>a,\*</sup>, Michael Bolte<sup>c</sup>, Safdar Hussain<sup>d</sup>, Noreen Hafeez<sup>e</sup>, Aurangzeb Hasan<sup>a,f</sup><sup>a</sup> Department of Chemistry, Quaid-i-Azam University, Islamabad 45320, Pakistan<sup>b</sup> Department of Biochemistry, Pir Mehr Ali Shah Arid Agriculture University, Rawalpindi, Pakistan<sup>c</sup> Institut für Anorganische Chemie, J.W. Goethe-Universität Frankfurt, Max-von-Laue-Str. 7, 60438 Frankfurt/Main, Germany<sup>d</sup> Department of Forensic Medicine & Toxicology, National University of Science and Technology, Islamabad 44000, Pakistan<sup>e</sup> Department of Forensic Medicine & Toxicology, IIMC, Riphah International University Islamabad, Pakistan<sup>f</sup> Department of Chemistry, Faculty of Science, University of Malaya, Kuala Lumpur 50603, Malaysia

## HIGHLIGHTS

- Pyrazolines are attractive drug scaffold with many biological applications.
- Synthesis of new pyrazoline derivatives equipped with *N*-acyl arms and long alkoxy side chains.
- Spectral, self-assembly, antifungal and anti-inflammatory studies.
- Effect of alkoxy chain length on molecular packing and bioactivity.

## GRAPHICAL ABSTRACT

A series of new pyrazoline derivatives equipped with *N*-acyl arms and long alkoxy groups as side chains was synthesized to investigate the effect of alkoxy chain length on molecular packing and bioactivity.

## ARTICLE INFO

## Article history:

Received 2 September 2013

Received in revised form 30 September 2013

Accepted 2 October 2013

Available online 14 October 2013

## Keywords:

Pyrazolines  
 Spectral characterization  
 Self assembly  
 Antifungal  
 Anti-inflammatory

## ABSTRACT

A series of new pyrazoline derivatives (**1b–4c**) bearing *N*-acyl arms and nine to twelve carbon long alkoxy side chains was synthesized and characterized on the basis of spectroscopic data and microanalysis. The nature of self-assembly to understand the interplay of alkoxy chain crystallization and various supramolecular interactions was investigated using single crystal X-ray diffraction studies. Interesting self-assembled supramolecular structures of **1b** and **4c** were observed in the crystal lattice owing to various  $CH \cdots O$ ,  $H \cdots H$ ,  $CH \cdots \pi$ , lonepair  $\cdots \pi$  and  $\pi \cdots \pi$  interactions. Further, all the synthesized compounds (**1b–4c**) were screened for their *in vitro* antifungal and anti-inflammatory activities. Compounds **2b**, **3b**, **2c** and **3c** showed significant to moderate antifungal activity against *Microsporum canis* whereas most of the other compounds were found inactive against all the five tested fungal strains. Good anti-inflammatory activity was observed for compounds **1b** with  $IC_{50}$  value 331  $\mu M$  compared to 273  $\mu M$  for Indomethacine, a standard reference drug. The bio-activity data demonstrates the relationship between lipophilicity, solubility and bioavailability.

© 2013 Elsevier B.V. All rights reserved.

## Introduction

Diversely substituted pyrazolines embedded with variety of functional groups represent a class of compounds of immense

\* Corresponding authors. Tel.: +92 333 5009600; fax: +92 51 90642241.

E-mail addresses: [profazmi@hotmail.com](mailto:profazmi@hotmail.com) (A. Abbas), [moazzam@qau.edu.pk](mailto:moazzam@qau.edu.pk) (M.M. Naseer).

importance in heterocyclic chemistry [1–6]. Pyrazoline ring is a dihydropyrazole having two adjacent nitrogen atoms and one endocyclic double bond. Considerable amount of research activity has been directed towards this class by the medicinal chemists. Among all its isomers, 2-pyrazoline has gained more attention due to its broad spectrum biological properties [7–9] and its presence in a number of pharmacologically important molecules such as azolid/tandearil (anti-inflammatory), phenazone/amidopyrene/methampyrone (analgesic and antipyretic), anturane (uricosuric) and indoxacarb (insecticidal). Therefore, a number of pharmacological activities [7–9] are documented in recent years for this class of compounds and still it is an active area of research [10–15].

The properties of solids are often governed by the way in which their constituent molecules are packed [16–23]. Therefore, understanding of the molecular packing is crucial in crystal engineering and structural chemistry to deliberately engineer the solid state materials of desired properties and functions. Both intra- and intermolecular interactions, such as hydrogen bonding, Van der Waals interaction,  $\text{CH}\cdots\pi$  and  $\pi\cdots\pi$  stacking play an important role in controlling the self-assembly of molecules in the crystal lattice [24–32]. However, the knowledge of intermolecular forces that hold the molecules in the solid state is still inadequate, offering a big challenge to the crystal engineers and supramolecular chemist's community to fully understand molecular packing and to pre-determine the self-assembly processes and properties of solids [33–36].

The interaction of drugs with biological systems depends on the ability of a particular drug to penetrate various biological membranes, tissues and barriers. Both lipophilicity of drug as physico-chemical parameter and composition of microbial membranes play an important role in the permeation of a drug through the microbial membranes for further drug action [37,38]. Owing to their structural diversity, easy access and tremendous importance, a series of new pyrazoline derivatives equipped with *N*-acyl arms and long alkoxy groups as side chains were chosen to investigate the effect of alkoxy chain length on molecular packing and bioactivity. The molecules were designed to understand the significance of the interplay of weak interactions and the role of alkoxy side chain toward the self-assembly in the solid state. Effect of alkoxy chains on antifungal and anti-inflammatory activities of the synthesized compounds was also investigated. The compounds of the present series as potential chelating agents may be good future candidates for the design of metal-based therapeutic agents with improved bioactivities.

## Experimental

### Materials and methods

All reagents and solvents were used as obtained from the supplier or recrystallized/redistilled as required. Thin layer chromatography (TLC) was performed using aluminum sheets (Merck) coated with silica gel 60 F<sub>254</sub>. Elemental analyses were carried out with a CHNS Analyzer, Model LECO-183. <sup>1</sup>H and <sup>13</sup>C NMR spectra of compounds were recorded with a Bruker 300 MHz spectrometer using deuterated solvents and TMS as internal standard. IR spectra of compounds were recorded on a Bio-Rad FTS 3000 MX spectrophotometer (400–4000 cm<sup>-1</sup>). The melting points of compounds were determined using capillary tubes and an electrothermal melting point apparatus, model MP-D Mitamura Riken Kogyo, Japan. *In vitro* anti-inflammatory and antifungal properties were studied at Panjwani Center for Molecular Medicine and Drug Research, International Center for Chemical Sciences, University of Karachi, Pakistan.

### General procedure for the synthesis of compounds (1a–4c)

The compounds (1a–4c) were synthesized following the previously reported procedure [39]. The carboxylic acid solution (25 ml) of the respective 4-alkoxychalcone (0.01 mol) containing a few drops of hydrochloric acid was heated at 60–65 °C for 30 min with constant stirring. Hydrazine hydrate (80%) (1.0 g, 0.02 mol) was then added dropwise to the reaction flask. After complete addition, the reaction mixture was heated to reflux for another 4–5 h. The reaction mixture was then cooled to room temperature and poured onto the crushed ice. The precipitates thus formed, were filtered, washed with distilled water and dried. The crude products were further purified by silica gel column chromatography using petroleum ether/ethyl acetate (4:1) as the mobile phase.

#### 1-Acetyl-3-phenyl-5-(4-nonyloxyphenyl)-2-pyrazoline (1b)

Yield 85%; yellowish white crystals; m.p. 78–81 °C; *R*<sub>f</sub> = 0.69 (petroleum ether:ethyl acetate, 4:1), FT-IR (KBr, cm<sup>-1</sup>) 1677 (s), 1648 (s), 1499 (s), 1295 (m), 1254 (s), 1050 (m), <sup>1</sup>H NMR (300 MHz, CDCl<sub>3</sub>) δ 0.90 (t, 3H, *J* = 7.2 Hz, —O—(CH<sub>2</sub>)<sub>8</sub>—CH<sub>3</sub>), 1.29–1.50 (m 12H, —O—CH<sub>2</sub>—CH<sub>2</sub>—(CH<sub>2</sub>)<sub>6</sub>—CH<sub>3</sub>), 1.77 (qn 2H, *J* = 7.8 Hz, —O—CH<sub>2</sub>—CH<sub>2</sub>—C<sub>7</sub>H<sub>15</sub>), 2.43 (s, 3H, O=C—CH<sub>3</sub>), 3.18 (dd, 1H, *J* = 4.8, 17.7 Hz, **H<sub>a</sub>**), 3.74 (dd, 1H, *J* = 12.0, 17.7 Hz, **H<sub>b</sub>**), 3.92 (t, 2H, *J* = 6.6 Hz, —O—CH<sub>2</sub>—), 5.57 (dd, 1H, *J* = 4.5, 11.7 Hz, **H<sub>x</sub>**), 6.85 (d, 2H, *J* = 8.7 Hz, ArH<sub>c=c</sub>), 7.17 (d, 2H, *J* = 8.7 Hz, ArH<sub>d=d</sub>), 7.44–7.47 (m, 3H, ArH<sub>f=f, g</sub>), 7.75–7.79 (m, 2H, ArH<sub>e=e</sub>), <sup>13</sup>C NMR (75 MHz, CDCl<sub>3</sub>) δ 14.1, 22.0, 22.6, 26.0, 29.1, 29.2, 29.3, 29.5, 31.8, 42.3, 59.4, 68.0, 114.7 (2C), 126.5 (2C), 126.9 (2C), 128.7 (2C), 130.2, 131.5, 133.8, 153.8, 158.6, 168.8, (EI) *m/z* (M<sup>+</sup>: 406, Base Peak 363). Anal. calcd. for C<sub>26</sub>H<sub>34</sub>N<sub>2</sub>O<sub>2</sub>: C, 76.81; H, 8.43; N, 6.89; Found: C, 76.77; H, 8.39; N, 6.96%.

#### 1-Acetyl-3-phenyl-5-(4-decyloxyphenyl)-2-pyrazoline (2b)

Yield 87%; yellowish white crystals; m.p. 81–83 °C; *R*<sub>f</sub> = 0.71 (petroleum ether:ethyl acetate, 4:1), FT-IR (KBr, cm<sup>-1</sup>) 1685 (s), 1637 (s), 1497 (s), 1293 (m), 1252 (s), 1049 (m), <sup>1</sup>H NMR (300 MHz, CDCl<sub>3</sub>) δ 0.90 (t, 3H, *J* = 7.0 Hz, —O—(CH<sub>2</sub>)<sub>9</sub>—CH<sub>3</sub>), 1.29–1.50 (m 14H, —O—CH<sub>2</sub>—CH<sub>2</sub>—(CH<sub>2</sub>)<sub>7</sub>—CH<sub>3</sub>), 1.77 (qn 2H, *J* = 7.0 Hz, —O—CH<sub>2</sub>—CH<sub>2</sub>—C<sub>8</sub>H<sub>17</sub>), 2.43 (s, 3H, O=C—CH<sub>3</sub>), 3.18 (dd, 1H, *J* = 4.5, 17.4 Hz, **H<sub>a</sub>**), 3.74 (dd, 1H, *J* = 12.0, 17.7 Hz, **H<sub>b</sub>**), 3.93 (t, 2H, *J* = 6.6 Hz, —O—CH<sub>2</sub>—), 5.57 (dd, 1H, *J* = 4.5, 11.7 Hz, **H<sub>x</sub>**), 6.84 (d, 2H, *J* = 8.7 Hz, ArH<sub>c=c</sub>), 7.17 (d, 2H, *J* = 8.7 Hz, ArH<sub>d=d</sub>), 7.44–7.47 (m, 3H, ArH<sub>f=f, g</sub>), 7.75–7.79 (m, 2H, ArH<sub>e=e</sub>), <sup>13</sup>C NMR (75 MHz, CDCl<sub>3</sub>) δ 14.1, 22.0, 22.6, 26.0, 29.2, 29.3, 29.5, 29.5, 31.9, 42.2, 59.4, 68.0, 114.7 (2C), 126.5 (2C), 126.9 (2C), 128.7 (2C), 130.2, 131.5, 133.8, 153.8, 158.6, 168.8, (EI) *m/z* (M<sup>+</sup>: 420, Base Peak 377). Anal. calcd. for C<sub>27</sub>H<sub>36</sub>N<sub>2</sub>O<sub>2</sub>: C, 77.10; H, 8.63; N, 6.66; Found: C, 77.03; H, 8.57; N, 6.73%.

#### 1-Acetyl-3-phenyl-5-(4-undecyloxyphenyl)-2-pyrazoline (3b)

Yield 88%; yellowish white crystals; m.p. 80–82 °C; *R*<sub>f</sub> = 0.68 (petroleum ether:ethyl acetate, 4:1), FT-IR (KBr, cm<sup>-1</sup>) 1683 (s), 1639 (s), 1495 (s), 1298 (m), 1251 (s), 1047 (m), <sup>1</sup>H NMR (300 MHz, CDCl<sub>3</sub>) δ 0.90 (t, 3H, *J* = 7.0 Hz, —O—(CH<sub>2</sub>)<sub>10</sub>—CH<sub>3</sub>), 1.28–1.50 (m 16H, —O—CH<sub>2</sub>—CH<sub>2</sub>—(CH<sub>2</sub>)<sub>8</sub>—CH<sub>3</sub>), 1.76 (qn 2H, *J* = 7.8 Hz, —O—CH<sub>2</sub>—CH<sub>2</sub>—C<sub>9</sub>H<sub>19</sub>), 2.43 (s, 3H, O=C—CH<sub>3</sub>), 3.18 (dd, 1H, *J* = 4.5, 17.7 Hz, **H<sub>a</sub>**), 3.74 (dd, 1H, *J* = 11.7, 17.7 Hz, **H<sub>b</sub>**), 3.92 (t, 2H, *J* = 6.6 Hz, —O—CH<sub>2</sub>—), 5.57 (dd, 1H, *J* = 4.5, 11.7 Hz, **H<sub>x</sub>**), 6.85 (d, 2H, *J* = 8.7 Hz, ArH<sub>c=c</sub>), 7.17 (d, 2H, *J* = 8.7 Hz, ArH<sub>d=d</sub>), 7.44–7.48 (m, 3H, ArH<sub>f=f, g</sub>), 7.75–7.79 (m, 2H, ArH<sub>e=e</sub>), <sup>13</sup>C NMR (75 MHz, CDCl<sub>3</sub>) δ 14.1, 22.0, 22.7, 26.0, 29.1, 29.2, 29.3, 29.3, 29.5, 29.6, 31.9, 42.2, 59.4, 68.0, 114.7 (2C), 126.5 (2C), 126.9 (2C), 128.7 (2C), 130.2, 131.5, 133.8, 153.8, 158.6, 168.8, (EI) *m/z* (M<sup>+</sup>: 434, Base Peak

391). Anal. calcd. for  $C_{28}H_{38}N_2O_2$ : C, 77.38; H, 8.81; N, 6.45; Found: C, 77.33; H, 8.75; N, 6.54%.

#### 1-Acetyl-3-phenyl-5-(4-dodecyloxyphenyl)-2-pyrazoline (**4b**)

Yield 83%; yellowish white crystals; m.p. 82–84 °C;  $R_f = 0.72$  (petroleum ether:ethyl acetate, 4:1), FT-IR (KBr,  $cm^{-1}$ ) 1684 (s), 1642 (s), 1491 (s), 1294 (m), 1258 (s), 1046 (m),  $^1H$  NMR (300 MHz,  $CDCl_3$ )  $\delta$  0.90 (t, 3H,  $J = 7.0$  Hz,  $-O-(CH_2)_{11}-CH_3$ ), 1.28–1.50 (m 18H,  $-O-CH_2-CH_2-(CH_2)_9-CH_3$ ), 1.76 (qn 2H,  $J = 7.5$  Hz,  $-O-CH_2-CH_2-C_{10}H_{21}$ ), 2.43 (s, 3H,  $O=C-CH_3$ ), 3.18 (dd, 1H,  $J = 4.5, 17.7$  Hz,  $H_a$ ), 3.74 (dd, 1H,  $J = 11.7, 17.7$  Hz,  $H_b$ ), 3.93 (t, 2H,  $J = 6.6$  Hz,  $-O-CH_2-$ ), 5.57 (dd, 1H,  $J = 4.5, 11.7$  Hz,  $H_x$ ), 6.84 (d, 2H,  $J = 8.7$  Hz,  $ArH_{c=c'}$ ), 7.17 (d, 2H,  $J = 8.7$  Hz,  $ArH_{d=d'}$ ), 7.44–7.49 (m, 3H,  $ArH_{f=f, g}$ ), 7.76–7.79 (m, 2H,  $ArH_{e=e'}$ ),  $^{13}C$  NMR (75 MHz,  $CDCl_3$ )  $\delta$  14.1, 22.0, 22.7, 26.0, 29.1, 29.2, 29.3, 29.3, 29.5, 29.5, 29.6, 31.9, 42.2, 59.4, 68.0, 114.7 (2C), 126.5 (2C), 126.9 (2C), 128.7 (2C), 130.2, 131.5, 133.8, 153.8, 158.6, 168.8 (EI)  $m/z$  ( $M^+$  448, Base Peak 405). Anal. calcd. for  $C_{29}H_{40}N_2O_2$ : C, 77.64; H, 8.99; N, 6.24; Found: C, 77.59; H, 8.91; N, 6.33%.

#### 1-Propionyl-3-phenyl-5-(4-nonyloxyphenyl)-2-pyrazoline (**1c**)

Yield 86%; yellowish white crystals; m.p. 71–74 °C;  $R_f = 0.71$  (petroleum ether:ethyl acetate, 4:1), FT-IR (KBr,  $cm^{-1}$ ) 1679 (s), 1645 (s), 1497 (s), 1291 (m), 1258 (s), 1053 (m),  $^1H$  NMR (300 MHz,  $CDCl_3$ )  $\delta$  0.91 (t, 3H,  $J = 7.0$  Hz,  $-O-(CH_2)_8-CH_3$ ), 1.21 (t, 3H,  $J = 7.5$  Hz,  $O=C-CH_2-CH_3$ ), 1.30–1.45 (m 12H,  $-O-CH_2-CH_2-(CH_2)_6-CH_3$ ), 1.77 (qn 2H,  $J = 7.8$  Hz,  $-O-CH_2-CH_2-C_7H_{15}$ ), 2.83 (q, 2H,  $J = 7.5$  Hz,  $O=C-CH_2-CH_3$ ), 3.17 (dd, 1H,  $J = 4.8, 17.7$  Hz,  $H_a$ ), 3.73 (dd, 1H,  $J = 11.7, 17.7$  Hz,  $H_b$ ), 3.93 (t, 2H,  $J = 6.6$  Hz,  $-O-CH_2-$ ), 5.55 (dd, 1H,  $J = 4.5, 11.7$  Hz,  $H_x$ ), 6.85 (d, 2H,  $J = 8.7$  Hz,  $ArH_{c=c'}$ ), 7.17 (d, 2H,  $J = 8.7$  Hz,  $ArH_{d=d'}$ ), 7.44–7.46 (m, 3H,  $ArH_{f=f, g}$ ), 7.76–7.79 (m, 2H,  $ArH_{e=e'}$ ),  $^{13}C$  NMR (75 MHz,  $CDCl_3$ )  $\delta$  9.0, 14.1, 22.6, 26.0, 27.6, 29.2, 29.3, 29.4, 29.5, 31.8, 42.0, 59.6, 67.9, 114.7 (2C), 126.5 (2C), 126.9 (2C), 128.7 (2C), 130.2, 131.6, 134.0, 153.5, 158.5, 172.2, (EI)  $m/z$  ( $M^+$  420, Base Peak 364). Anal. calcd. for  $C_{27}H_{36}N_2O_2$ : C, 77.10; H, 8.63; N, 6.66; Found: C, 77.03; H, 8.58; N, 6.74%.

#### 1-Propionyl-3-phenyl-5-(4-decyloxyphenyl)-2-pyrazoline (**2c**)

Yield 83%; yellowish white crystals; m.p. 67–69 °C;  $R_f = 0.69$  (petroleum ether:ethyl acetate, 4:1), FT-IR (KBr,  $cm^{-1}$ ) 1684 (s), 1639 (s), 1495 (s), 1295 (m), 1257 (s), 1048 (m),  $^1H$  NMR (300 MHz,  $CDCl_3$ )  $\delta$  0.91 (t, 3H,  $J = 7.0$  Hz,  $-O-(CH_2)_9-CH_3$ ), 1.21 (t, 3H,  $J = 7.8$  Hz,  $O=C-CH_2-CH_3$ ), 1.29–1.47 (m 14H,  $-O-CH_2-CH_2-(CH_2)_7-CH_3$ ), 1.77 (qn 2H,  $J = 7.8$  Hz,  $-O-CH_2-CH_2-C_8H_{17}$ ), 2.83 (q, 2H,  $J = 7.5$  Hz,  $O=C-CH_2-CH_3$ ), 3.17 (dd, 1H,  $J = 4.8, 17.7$  Hz,  $H_a$ ), 3.73 (dd, 1H,  $J = 12.0, 17.7$  Hz,  $H_b$ ), 3.93 (t, 2H,  $J = 6.6$  Hz,  $-O-CH_2-$ ), 5.55 (dd, 1H,  $J = 4.5, 11.7$  Hz,  $H_x$ ), 6.84 (d, 2H,  $J = 8.7$  Hz,  $ArH_{c=c'}$ ), 7.17 (d, 2H,  $J = 8.7$  Hz,  $ArH_{d=d'}$ ), 7.44–7.47 (m, 3H,  $ArH_{f=f, g}$ ), 7.76–7.80 (m, 2H,  $ArH_{e=e'}$ ),  $^{13}C$  NMR (75 MHz,  $CDCl_3$ )  $\delta$  9.0, 14.1, 22.6, 26.0, 27.6, 29.2, 29.3, 29.3, 29.5, 29.5, 31.9, 42.0, 59.6, 68.0, 114.7 (2C), 126.5 (2C), 126.9 (2C), 128.7 (2C), 130.2, 131.6, 134.0, 153.5, 158.5, 172.2, (EI)  $m/z$  ( $M^+$  434, Base Peak 378). Anal. calcd. for  $C_{28}H_{38}N_2O_2$ : C, 77.38; H, 8.81; N, 6.45; Found: C, 77.32; H, 8.77; N, 6.53%.

#### 1-Propionyl-3-phenyl-5-(4-undecyloxyphenyl)-2-pyrazoline (**3c**)

Yield 87%; yellowish white crystals; m.p. 72–75 °C;  $R_f = 0.73$  (petroleum ether:ethyl acetate, 4:1), FT-IR (KBr,  $cm^{-1}$ ) 1683 (s), 1632 (s), 1498 (s), 1297 (m), 1259 (s), 1053 (m),  $^1H$  NMR (300 MHz,  $CDCl_3$ )  $\delta$  0.90 (t, 3H,  $J = 7.0$  Hz,  $-O-(CH_2)_{10}-CH_3$ ), 1.20 (t, 3H,  $J = 7.8$  Hz,  $O=C-CH_2-CH_3$ ), 1.28–1.47 (m 16H,  $-O-CH_2-CH_2-(CH_2)_8-CH_3$ ), 1.76 (qn 2H,  $J = 7.5$  Hz,  $-O-CH_2-CH_2-C_9H_{19}$ ), 2.83 (q, 2H,  $J = 7.5$  Hz,  $O=C-CH_2-CH_3$ ), 3.17 (dd, 1H,  $J = 4.8, 17.7$  Hz,  $H_a$ ), 3.73 (dd, 1H,  $J = 12.0, 17.7$  Hz,  $H_b$ ), 3.92 (t, 2H,  $J = 6.6$  Hz,  $-O-CH_2-$ ), 5.55 (dd, 1H,  $J = 4.5, 11.7$  Hz,  $H_x$ ), 6.84 (d, 2H,

$J = 8.7$  Hz,  $ArH_{c=c'}$ ), 7.17 (d, 2H,  $J = 8.7$  Hz,  $ArH_{d=d'}$ ), 7.44–7.47 (m, 3H,  $ArH_{f=f, g}$ ), 7.76–7.80 (m, 2H,  $ArH_{e=e'}$ ),  $^{13}C$  NMR (75 MHz,  $CDCl_3$ )  $\delta$  9.0, 14.1, 22.7, 26.0, 27.6, 29.2, 29.3, 29.3, 29.4, 29.5, 29.6, 31.9, 42.0, 59.6, 67.9, 114.7 (2C), 126.5 (2C), 126.9 (2C), 128.7 (2C), 130.2, 131.6, 134.0, 153.5, 158.5, 172.2, (EI)  $m/z$  ( $M^+$  448, Base Peak 392). Anal. calcd. for  $C_{29}H_{40}N_2O_2$ : C, 77.64; H, 8.99; N, 6.24; Found: C, 77.58; H, 8.92; N, 6.32%.

#### 1-Propionyl-3-phenyl-5-(4-dodecyloxyphenyl)-2-pyrazoline (**4c**)

Yield 82%; yellowish white crystals; m.p. 70–73 °C;  $R_f = 0.70$  (petroleum ether:ethyl acetate, 4:1), FT-IR (KBr,  $cm^{-1}$ ) 1687 (s), 1647 (s), 1497 (s), 1296 (m), 1254 (s), 1051 (m),  $^1H$  NMR (300 MHz,  $CDCl_3$ )  $\delta$  0.91 (t, 3H,  $J = 7.0$  Hz,  $-O-(CH_2)_{11}-CH_3$ ), 1.21 (t, 3H,  $J = 7.5$  Hz,  $O=C-CH_2-CH_3$ ), 1.29–1.47 (m 18H,  $-O-CH_2-CH_2-(CH_2)_9-CH_3$ ), 1.77 (qn 2H,  $J = 7.5$  Hz,  $-O-CH_2-CH_2-C_{10}H_{21}$ ), 2.83 (q, 2H,  $J = 7.5$  Hz,  $O=C-CH_2-CH_3$ ), 3.17 (dd, 1H,  $J = 4.5, 17.7$  Hz,  $H_a$ ), 3.73 (dd, 1H,  $J = 11.7, 17.7$  Hz,  $H_b$ ), 3.93 (t, 2H,  $J = 6.6$  Hz,  $-O-CH_2-$ ), 5.55 (dd, 1H,  $J = 4.5, 11.7$  Hz,  $H_x$ ), 6.83 (d, 2H,  $J = 8.7$  Hz,  $ArH_{c=c'}$ ), 7.17 (d, 2H,  $J = 8.7$  Hz,  $ArH_{d=d'}$ ), 7.44–7.47 (m, 3H,  $ArH_{f=f, g}$ ), 7.75–7.80 (m, 2H,  $ArH_{e=e'}$ ),  $^{13}C$  NMR (75 MHz,  $CDCl_3$ )  $\delta$  14.1, 22.7, 26.0, 27.6, 29.2, 29.3, 29.3, 29.5, 29.6, 29.6, 29.6, 31.9, 42.0, 59.6, 68.0, 68.1, 114.7 (2C), 126.5 (2C), 126.9 (2C), 128.7 (2C), 130.1, 131.6, 134.0, 153.5, 158.5, 172.2, (EI)  $m/z$  ( $M^+$  462, Base Peak 406). Anal. calcd. for  $C_{30}H_{42}N_2O_2$ : C, 77.88; H, 9.15; N, 6.05; Found: C, 77.82; H, 9.09; N, 6.13%.

#### Single crystal X-ray crystallography

##### Data collection and structural refinement of **1b** and **4c**

In order to investigate the effect of alkoxy chain on solid state self assembly, the single crystals of compound **1b** and **4c** were grown in ethanolic solution. The pale yellow crystals were mounted in random orientation on a glass fiber on a Stoe IPDS-II two circle diffractometer [40] equipped with graphite monochromated Mo  $K\alpha$  radiation ( $k = 0.71073$  Å). The structure was solved by direct methods using SHELXS97 and refined with full-matrix least-squares on F2 with SHELXL-97 [41]. All non-hydrogen atoms were refined anisotropically. Hydrogen atoms were located in a difference map but refined using a riding model. The crystal data and refinement details are summarized in Table 1.

#### Biological activity

##### Antifungal studies (in vitro)

All compounds were studied against six fungal cultures for anti-fungal activities. Sabouraud dextrose agar (SDA) (Oxoid, Hampshire, England) was seeded with  $10^5$  (cfu)  $mL^{-1}$  fungal spore suspensions and transferred to Petri plates. Discs soaked in 20 mL (200  $\mu g/mL$  in DMSO) of each compound were placed at different positions on the agar surface. The plates were incubated at 32 °C for 7 days. The results were recorded as % of inhibition and compared with standard reference drugs miconazole and amphotericin B.

**Assay procedure (agar tube dilution).** Test tubes were marked up to 10 cm from the base. Then 4 mL volume of SDA was poured into screw-capped tubes or cotton plugged test tubes and was autoclaved at 121 °C. Test tubes were allowed to cool down to 50 °C and non-solidified SDA was loaded with 67  $\mu L$  of test compound to obtain a concentration of 200  $\mu g/mL$ . Test tubes were then allowed to solidify in slanting position at room temperature. Test tubes were prepared in triplicates for each fungal species. Test tubes containing solidified media and test compound were inoculated with 4 mm diameter piece of inoculum taken from a 7 days old culture of fungus. Positive and negative control test tubes were also inoculated with Miconazole/Amphotericin B and DMSO

**Table 1**  
Crystallographic data for **1b** and **4c**.

Crystal data	<b>1b</b>	<b>4c</b>
Chemical formula	C <sub>26</sub> H <sub>34</sub> N <sub>2</sub> O <sub>2</sub>	C <sub>30</sub> H <sub>42</sub> N <sub>2</sub> O <sub>2</sub>
M <sub>r</sub>	406.55	462.66
Crystal system, space group	Triclinic, P1	Monoclinic, P2 <sub>1</sub> /c
Temperature (K)	173	173
a, b, c (Å)	6.2697 (6), 7.3333 (7), 27.826 (3)	5.3072 (4), 28.2115 (15), 18.4326 (13)
α, β, γ (°)	86.588 (8), 86.561 (8), 64.862 (7)	95.479 (6)
V (Å <sup>3</sup> )	1155.3 (2)	2747.2 (3)
Z	2	4
Radiation type	Mo Kα	Mo Kα
μ (mm <sup>-1</sup> )	0.07	0.07
Crystal size (mm)	0.22 × 0.13 × 0.12	0.32 × 0.14 × 0.13
<i>Data collection</i>		
Diffractometer	STOE IPDS II two-circle-diffractometer	STOE IPDS II two-circle-diffractometer
Absorption correction	–	–
No. of measured, independent and Observed [I > 2σ(I)] reflections	11042, 4148, 3141	26062, 4980, 3143
R <sub>int</sub>	0.058	0.083
(sin θ/λ) <sub>max</sub> (Å <sup>-1</sup> )	0.599	0.601
<i>Refinement</i>		
R[F <sup>2</sup> > 2σ(F <sup>2</sup> )], wR(F <sup>2</sup> ), S	0.041, 0.108, 0.96	0.043, 0.105, 0.88
No. of reflections	4148	4980
No. of parameters	274	308
No. of restraints	0	0
H-atom treatment	H-atom parameters constrained	H-atom parameters constrained
Δ <sub>max</sub> , Δ <sub>min</sub> (e Å <sup>-3</sup> )	0.14, -0.19	0.21, -0.21

respectively. The whole procedure was carried out in laminar flow hood (LFH) under strict sterile conditions. Test tubes were incubated at 28 °C during 7 days. Cultures were examined twice a week during the incubation period. Reading was taken by measuring the linear length of fungus in slant by measuring growth (mm) and growth inhibition was calculated with reference to negative control. Percentage inhibition of fungal growth for each concentration of compound was determined by using the following formula:

Percentage inhibition of fungal growth

$$= 100 - \frac{\text{Linear growth in test (mm)}}{\text{Linear growth in control (mm)}} \times 100$$

#### Anti-inflammatory studies (in vitro)

**Isolation of human neutrophils.** Inflammation occurs as a defensive response, which induces physiological adaptations to limit tissue damage and removes the pathogenic infection. Reactive oxygen species (ROS) are formed subsequent to the assembly and activation of the phagocyte-specific enzyme, NADPH Oxidase. This process is initiated by the production of superoxide anion during a 'respiratory burst' of non-mitochondrial oxygen uptake by an NADPH oxidase system. This study used the water-soluble tetrazolium salt (WST-1) to measure superoxide production by neutrophils activated by opsonized zymosan, which induces phagocytic activation of neutrophils. This technique is more sensitive and reliable as compared to other available techniques.

**Respiratory burst assay.** Anti-inflammatory activity of the compounds was determined by using a modified assay of Tan and Berridge [42]. This *in vitro* assay was based on the reduction of highly water-soluble tetrazolium salt (WST-1) in the presence of activated neutrophils. Anti-inflammatory activity was determined in a total volume of 200 μL MHS (pH 7.4) containing 1.0–104 neutrophils/mL, 250 μM WST-1 and various concentrations of test compounds. The control contained buffer, neutrophils and WST-1. All compounds were equilibrated at 37 °C and the reaction was initiated by adding opsonized zymosan A (15 mg/mL), which was prepared by mixing with human pooled

serum, followed by centrifugation at 3000 rpm whereby the pellet was resuspended in PBS buffer. Absorbance was measured at 450 nm. Aspirin and indomethacin were used as positive controls which are widely used as non-steroidal anti-inflammatory drugs (NSAIDs) for the treatment of several inflammatory diseases. The IC<sub>50</sub> values were calculated by comparison with the DMSO taken as blank and expressed as the percent inhibition of superoxide anions produced. The percent inhibitory activity by the samples was determined against a DMSO blank and calculated using the following formula:

$$\% \text{ Inhibition} = 100 - \left[ \frac{\text{OD Test Compound}}{\text{OD Control}} \right] \times 100$$

IC<sub>50</sub> of samples was determined by using EZ-FIT Windows-based software.

## Results and discussion

### Chemistry

The compounds (**1b–4c**) were synthesized by reacting equimolar quantities of (*E*)-3-(4-alkyloxyphenyl)-1-phenylprop-2-en-1-ones (**1a–4a**) and hydrazine in glacial acetic acid/propionic acid solvent containing catalytic amount of hydrochloric acid (**Scheme 1**) and purified by silica gel column chromatography using petroleum ether/ethyl acetate as mobile phase. All the products were obtained as solids in 82–88% yield. The structures of all the compounds were established on the basis of spectroscopic data and microanalysis. The three dimensional structure of the new pyrazoline derivatives was further proved unambiguously by the single crystal X-ray diffraction analysis of **1b** and **4c**.

### Spectroscopic characterization of **1b–4c**

#### IR spectra

In the IR spectra of compounds (**1b–4c**), a sharp band at 1648–1637 cm<sup>-1</sup> and 1687–1679 cm<sup>-1</sup> was assigned to the stretching of ν(C=N) and ν(C=O), respectively. The carbon–nitro-

gen single bond (C–N) stretching frequencies were observed at 1297–1291  $\text{cm}^{-1}$ . The presence of these frequencies suggests the formation of cyclic pyrazoline ring. Two strong bands at stretching frequencies in the range of 1259–1251  $\text{cm}^{-1}$  and 1053–1046  $\text{cm}^{-1}$  indicate the presence of Ar–O–R group.

### $^1\text{H}$ NMR spectra

$^1\text{H}$  NMR spectral data for all *N*-acyl pyrazolines recorded in  $\text{CDCl}_3$  along with their possible assignments is reported in the experimental section. All the protons due to pyrazoline and aromatic rings were found in their expected chemical shift regions. The formation of the five membered pyrazoline ring was established by the presence of two methylene protons ( $\text{H}_a$  and  $\text{H}_b$ ) and one methine proton ( $\text{H}_x$ ) as three doublet of doublets. The singlets for methyl protons of acetyl group ( $\text{O}=\text{C}-\text{CH}_3$ ) in compounds **1b–4b** were observed at 2.43 ppm, whereas a triplet and quartet at 1.20–1.21 and 2.83 ppm was noticed for methyl protons ( $\text{O}=\text{C}-\text{CH}_2-\text{CH}_3$ ) and the methylene protons ( $\text{O}=\text{C}-\text{CH}_2-\text{CH}_3$ ), respectively for propionyl group in compounds **1c–4c**. In addition, a triplet was observed at 3.92–3.93 ppm for the methylenic protons ( $\text{Ar}-\text{O}-\text{CH}_2-$ ) of the alkoxy chain directly attached to the oxygen atom. All other protons of alkoxy chain appeared in the range of 0.9–1.77 ppm. The conclusions drawn from the  $^1\text{H}$  NMR data provided further support to the observations of presence of different functional groups discussed in IR section (Fig. 1).

### $^{13}\text{C}$ NMR spectra

The  $^{13}\text{C}$  NMR spectra of compounds (**1b–4c**) displayed peaks at 67.9–68.0 ppm, 42.0–42.3 ppm and 59.4–59.6 ppm for  $\text{C}_3$ ,  $\text{C}_4$  and  $\text{C}_5$  carbons, respectively. All the aromatic carbons were observed in the range of 114.7–158.6 ppm. The signals for acyl carbons were noticed in the range of 168.8–172.2 ppm for all the compounds. Furthermore, the results of  $^{13}\text{C}$  NMR data were found to be in good agreement with the results of IR and  $^1\text{H}$  NMR spectra of these compounds.

### Mass spectra

The electron impact mass spectra (EIMS) of the all the synthesized pyrazoline derivatives **1b–4c** are presented in the experimental part. The mass spectral data and fragmentation pattern of all the synthesized 2-pyrazoline derivatives [39,43], clearly justify the formation of proposed structures discussed in IR,  $^1\text{H}$  and  $^{13}\text{C}$  NMR spectroscopy. Further, a molecular ion peak ( $\text{M}^+$ ) was observed for all the compounds at their respective molecular masses. The most stable fragments or base peaks were observed by the loss of *N*-acyl fragment as radical. The proposed mass fragmentation pattern of the representative compound **1b** where molecular ion

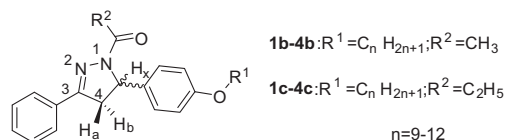


Fig. 1. Labelling scheme of protons of compounds **1b–4c**.

peak appeared at  $m/z$  406 (Calcd. 406.26) of  $[\text{C}_{26}\text{H}_{34}\text{N}_2\text{O}_2]^+$  and most stable fragment at  $m/z$  363 (Calcd. 363.24) of  $[\text{C}_{24}\text{H}_{31}\text{N}_2\text{O}]^+$  is shown in Fig. 2.

### Solid state self-assembly

The self-assembly studies were also carried out to identify the structural features that govern the molecular alignment in the solid state and to understand the interplay of alkoxy chains crystallization and various supramolecular interactions, using single crystal X-ray diffraction studies. For this purpose, good quality single crystals of only two compounds **1b** and **4c** were grown. Selected crystal data and structural refinement parameters of compound **1b** and **4c** are given in Table 1. All our attempts to cultivate single crystals for other compounds for these studies were unsuccessful.

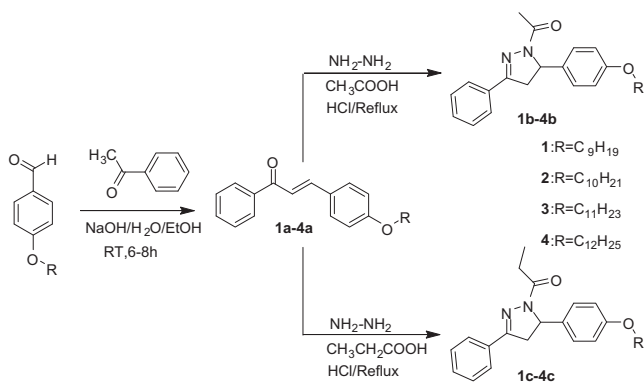
### Crystal structure of **1b**

Single crystals of **1b** were obtained from ethanol solution using slow evaporation of solvent at ambient conditions and were found to have a triclinic crystal lattice with the  $P1$  space group. The ORTEP representation and atom labeling scheme of the compound **1b** is shown in Fig. 3. The central pyrazoline unit is nearly in the same plane as the phenyl ring at its 3-position, making a dihedral angle of 1.88° [ $\text{C}(16)-\text{C}(11)-\text{C}(3)-\text{N}(2)$ ]. The alkoxy substituted aryl ring present on asymmetric carbon of pyrazoline ring is oriented in such a way that one of its hydrogen is located on top of the pyrazoline ring at a distance 2.683 Å from the centre of pyrazoline ring. The angles around asymmetric carbons are 100.49° [ $\text{C}(4)-\text{C}(5)-\text{N}(1)$ ], 111.07° [ $\text{C}(21)-\text{C}(5)-\text{N}(1)$ ], 114.80° [ $\text{C}(4)-\text{C}(5)-\text{C}(21)$ ] and 110.00° [ $\text{C}(21)-\text{C}(5)-\text{H}(5)$ ]. In the pyrazoline ring, the C–N, C=N and N–N bond lengths are 1.483 Å, 1.293 Å and 1.394 Å, respectively.

Fig. 4 shows the molecular packing of **1b** in which two independent molecules present in asymmetric unit form 1D-supramolecular chains. The long alkoxy group of 1D-supramolecular chain structure move in face to face parallel fashion but opposite to its neighboring 1D-supramolecular chain present in the same asymmetric unit. These 1D-supramolecular chains with alkoxy groups running in opposite direction are stacked on each other in the crystal lattice to provide highly packed supramolecular structure (Fig. 4a). This structure is stabilized by  $\text{CH}\cdots\text{O}$ ,  $\text{CH}\cdots\pi$  and  $\text{H}\cdots\text{H}$  [44] interactions. Each individual molecule of the chain is connected to its neighboring molecule by  $\text{CH}\cdots\text{O}$  [ $\text{C}(13)-\text{H}(13)\cdots\text{O}(1)$  2.606 Å] and  $\text{H}\cdots\text{H}$  [ $\text{C}(14)-\text{H}(14)\cdots\text{H}(7A)$  2.350 Å] interactions (Fig. 4b). These supramolecular 1D chains are stacked on top of each other utilizing  $\text{CH}\cdots\text{O}$  [ $\text{C}(22)-\text{H}(22)\cdots\text{O}(1)$  2.412 Å],  $\text{CH}\cdots\pi$  [ $\text{C}(13)-\text{H}(13)\cdots\text{C}(22)$  2.892 Å] and  $\text{H}\cdots\text{H}$  [ $\text{C}(25)-\text{H}(25)\cdots\text{H}(31B)$  2.396 Å] interactions (Fig. 4c).

### Crystal structure of **4c**

The good quality single crystals of **4c** were grown in similar conditions to **1b** and were found to have a monoclinic crystal lattice with the  $P2_1/c$  space group. The ORTEP representation and atom labeling scheme of the compound **4c** is shown in Fig. 5. The central pyrazoline unit is slightly out of plane of the phenyl ring at its 3-position as compared to **1b**, making a dihedral angle of



Scheme 1. Synthesis of new *N*-acyl pyrazolines **1b–4c**.

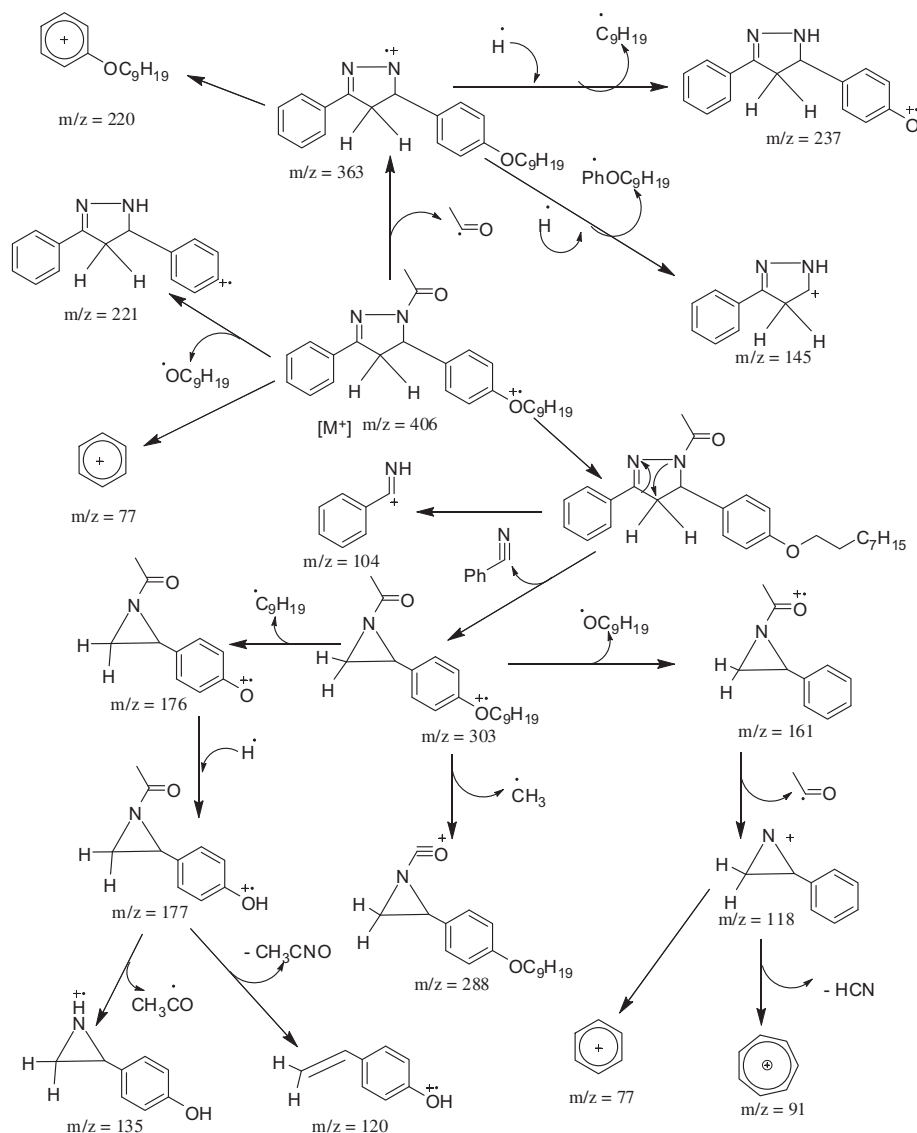


Fig. 2. Mass fragmentation pattern of **1b**.

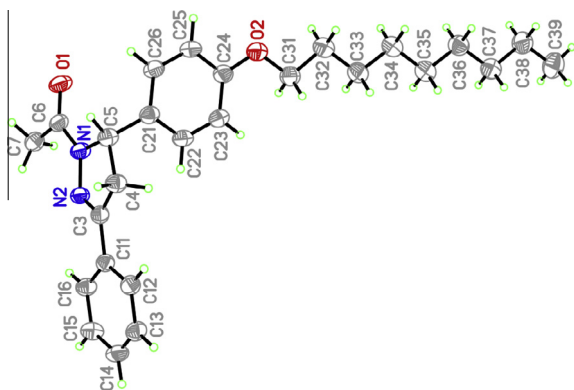
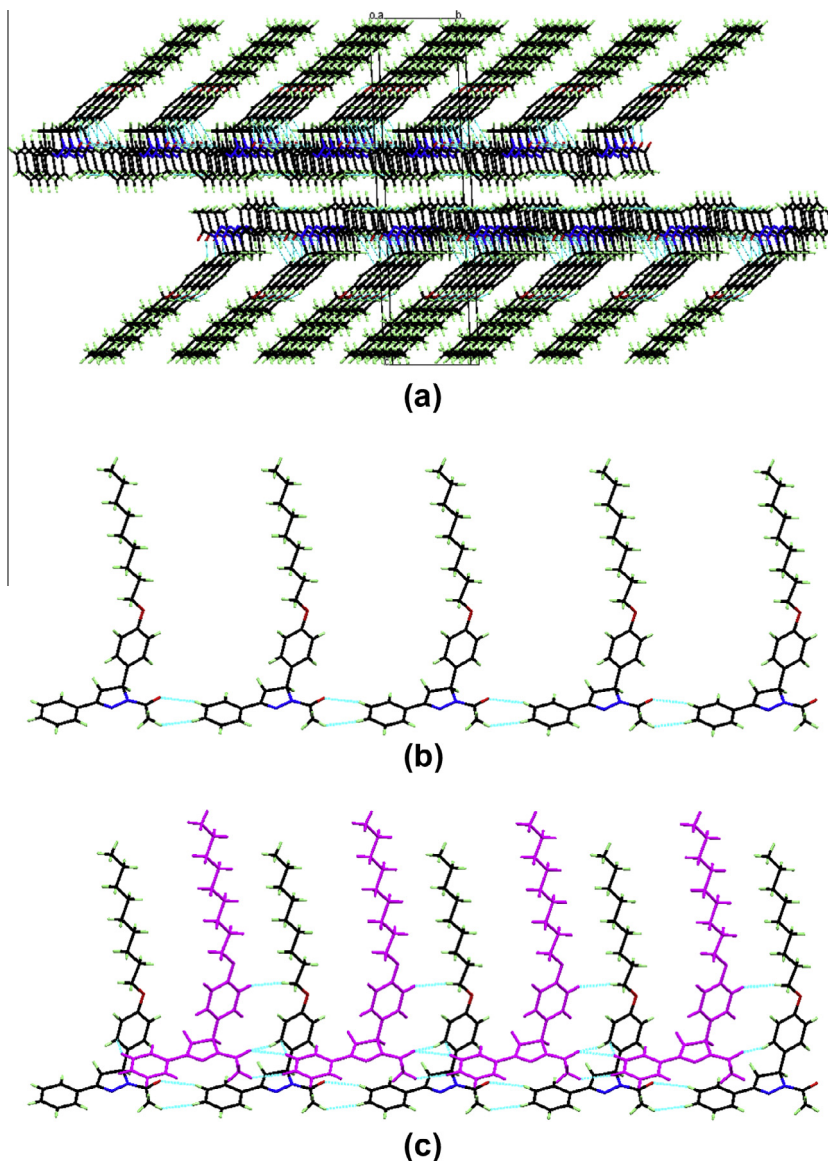


Fig. 3. The ORTEP diagram and atom labeling scheme of **1b**.

4.58° [C(16)–H(11)–C(3)–N(2)]. Similarly, alkoxy substituted aryl ring on asymmetric carbon of pyrazoline ring is also slightly tilted as compared to **1b**, not located exactly at the top of pyrazoline ring. The distance from the center of pyrazoline ring and H(22) of alkoxy

substituted aromatic ring was measured to be 2.870 Å as compared to 2.683 Å for **1b**. The angles around asymmetric carbons are 101.08° [C(4)–C(5)–N(1)], 112.98° [C(21)–C(5)–N(1)], 115.16° [C(4)–C(5)–C(21)] and 109.10° [C(21)–C(5)–H(5)]. In the pyrazoline ring, the C–N, C=N and N–N bond lengths are 1.475 Å, 1.290 Å and 1.388 Å, respectively.

Fig. 6 shows the molecular packing of **4c** which also shows stacked 1D-supramolecular chains. However, this structure is different from **1b**. Unlike **1b**, the alkoxy substitution on individual molecules of each supramolecular chain moves in alternate fashion in the crystal lattice. Interestingly, two neighboring 1D-supramolecular chains of **4c** are packed with interdigitation of alkoxy chains in a V/inverted V manner (Fig. 6a). These 1D-supramolecular chains are stacked on each other in a way similar to **1b**. The stacked supramolecular structure of **4c** is stabilized by various CH···O, lonepair···π [45], CH···π and π···π interactions. Each individual molecule of the supramolecular chain is connected to its neighboring molecule by two different CH···O [C(13)–H(13)···O(6) 2.563 Å, C(14)–H(14)···O(6) 2.663 Å] and lonepair···π [O(6)···H(13) 3.209 Å] contacts (Fig. 6b), whereas CH···π [C(5)–H(5)···C(11) 2.821 Å], π···π [C(3)···C(15) 3.395 Å] and CH···π [C(31)–H(31A)···C(16) 2.854 Å] interactions are uti-



**Fig. 4.** (a) Stacked 3D-supramolecular structure of **1b** view along *a*-axis. (b) An infinite 1D-supramolecular chain of **1b** stabilized by CH...O [C(13)—H(13)...O(1) 2.606 Å] and H...H [C(14)—H(14)...H(7A) 2.350 Å] interactions viewed along *a*-axis. (c) Two successive stacked supramolecular chains of **1b** viewed along *a*-axis stabilized by CH...O [C(22)—H(22)...O(1) 2.412 Å], CH... $\pi$  [C(13)—H(13)...C(22) 2.892 Å] and H...H [C(25)—H(25)...H(31B) 2.396 Å] interactions.

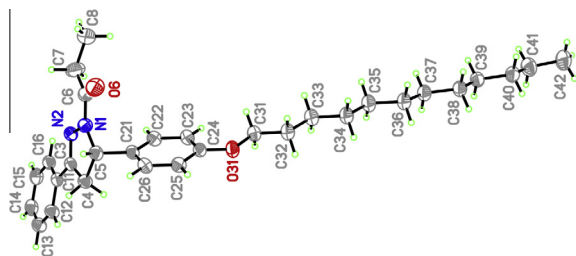


**Fig. 5.** The ORTEP diagram and atom labeling scheme of **4c**.

lized to stabilize stacking of supramolecular chains on one another (Fig. 6c). It is important to mention here that this kind of structural units stabilized by a number of supramolecular interactions represents and exemplify a unique pattern of self-assembly. These compounds are fluorescent and organic fluorescent materials are used in a wide range of applications, like electronic display devices,

cosmetics, surface coatings, inks and textile industries [39]. In addition, these compounds having long alkoxy chains are potential candidates for liquid crystalline studies.

#### Biological activity

##### Antifungal studies (in vitro)

The antifungal screening of all the synthesized compounds (**1b–4c**) was carried out against *Candida albicans* (A), *Aspergillus flavus* (B), *Microsporium canis* (C), *Fusarium solani* (D), and *Candida glabrata* (E) fungal strains according to the literature protocol [46]. Four out of eight compounds showed moderate to significant antifungal activity (50–80% inhibition) against *Microsporium canis* (C). Compound **2b** was found to be the most active with 80% inhibition against *Microsporium canis* (C). Compounds **1b**, **3b** and **3c** also showed  $\geq 30\%$  inhibition against *Fusarium solani*. However, most of the other compounds either showed no activity or weak activity against one or more of the tested fungal strains. It is generally true

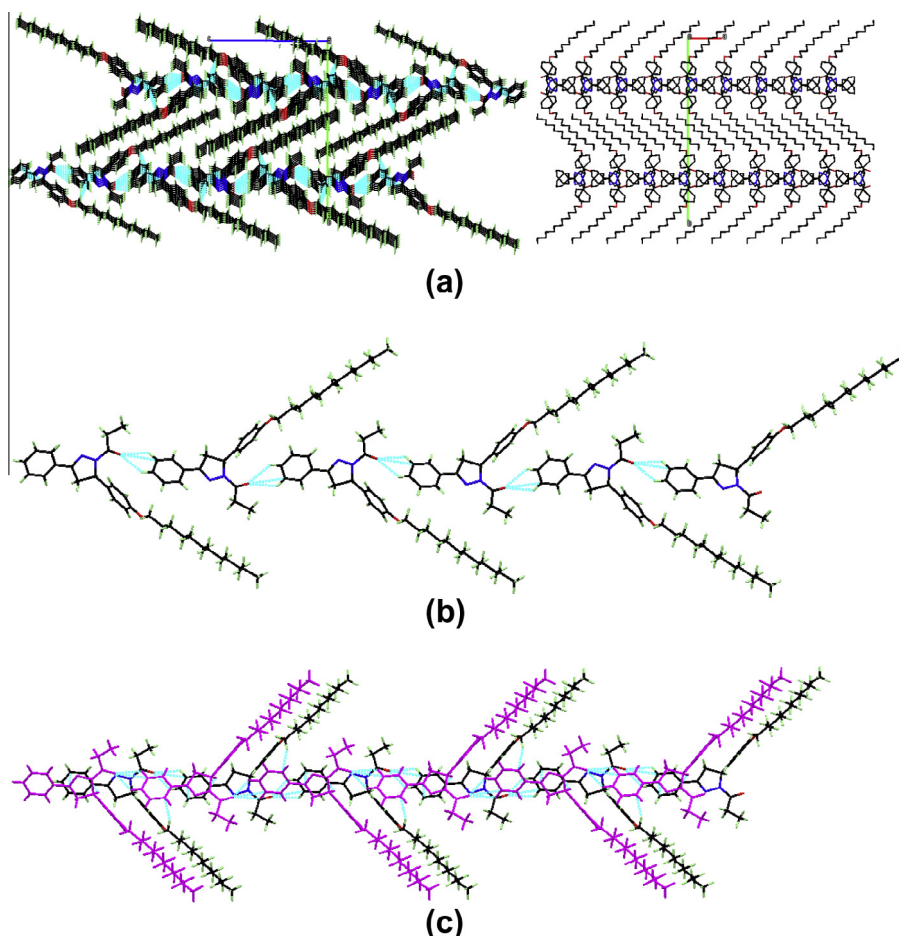


**Fig. 6.** (a) Stacked 3D-supramolecular structure of **4c** viewed along *a*-axis (left) and *c*-axis (right). (b) An infinite 1D-supramolecular chain of **4c** viewed along *a*-axis stabilized by CH...O [C(13)—H(13)...O(6) 2.563 Å, C(14)—H(14)...O(6) 2.663 Å] and a lonepair...π [O(6)...H(13) 3.209 Å] contacts. (c) Two successive stacked supramolecular chains of **4c** viewed along *a*-axis stabilized by CH...π [C(5)—H(5)...C(11) 2.821 Å], π...π [C(3)...C(15) 3.395 Å] and CH...π [C(31)—H(31A)...C(16) 2.854 Å] interactions.

that by increasing the lipophilic character, bioactivity of the compounds also increases due to their greater permeation through the lipid layer of the membrane. However, for the present series, it is interesting to note that compounds bearing nine and ten carbon alkoxy chains were found to be more active as compared to compounds with shorter or longer alkyl chains. This trend may be attributed to lesser lipophilicity of compounds bearing shorter alkoxy chain and poor solubility of compounds bearing longer alkoxy chain in the DMSO solvent, which is used for this bioassay or it may be credited to different conformational arrangements of alkoxy chains. The results of antifungal activities (%inhibition) were compared with standard reference drugs miconazole and amphotericin B and are presented in Table 2. The results of this *in vitro* study demonstrate the relationship between lipophilicity, solubility and bioavailability.

#### Antiinflammatory studies (*in vitro*)

The novel series of *N*-acyl-2-pyrazolines (**1b–4c**) was also screened for their anti-inflammatory activity. The results of this study were compared with standard reference drug-Indomethacine and are summarized in Table 3. The anti-inflammatory activity of all the tested compounds was first evaluated in terms of percent growth inhibition. The compounds which showed  $\geq 70\%$  inhibition were retested and the results were expressed as  $IC_{50}$  (inhibitory concentration 50%), the concentration of the compound which inhibits the inflammation by 50% of three independent experiments. In the present series, only com-

pound **1b** showed good anti-inflammatory activity with  $IC_{50}$  value 331  $\mu\text{M}$  as compared to 273  $\mu\text{M}$  for Indomethacine. All other compounds showed low anti-inflammatory activity. In literature, different mechanisms are proposed for anti-inflammatory agents to explain their *in vitro/in vivo* mode of action [47]. However, no general mechanism is reported so far. They probably have multiple cellular mechanisms acting on multiple sites of cellular infrastructure.

**Table 2**  
Antifungal bioassay of compounds **1b–4c**.

Compd.	% Inhibition (at conc. 200 $\mu\text{g}/\text{mL}$ )					Activity profile
	(A)	(B)	(C)	(D)	(E)	
<b>1b</b>	00	10	10	40	00	Negative
<b>2b</b>	00	00	<b>80</b>	00	00	<b>Positive</b>
<b>3b</b>	00	00	<b>70</b>	30	00	<b>Positive</b>
<b>4b</b>	00	00	10	20	00	Negative
<b>1c</b>	00	00	00	20	00	Negative
<b>2c</b>	00	00	<b>50</b>	00	00	<b>Positive</b>
<b>3c</b>	00	00	<b>50</b>	30	00	<b>Positive</b>
<b>4c</b>	00	00	10	00	00	Negative
<b>MICON<sup>a</sup></b>	108	–	98	73	110	<b>Positive</b>
<b>AMPHO<sup>b</sup></b>	–	20	–	–	–	Negative

Note: Bold values represent significant results.

<sup>a</sup> MICON: miconazole.

<sup>b</sup> AMPHO: amphotericin B. (A): *candida albicans*; (B): *aspergillus flavus*; (C): *microsporium canis*; (D): *fusarium solani*; (E): *candida glabrata*.

**Table 3**  
Anti-inflammatory activity of **1b–4c**.

Compd.	R <sup>1</sup>	R <sup>2</sup>	% Inhibition and IC <sub>50</sub>		Activity profile
			% Inhibition (at 500 μM)	IC <sub>50</sub> ± SEM (μM)	
<b>1b</b>	C <sub>9</sub> H <sub>19</sub>	CH <sub>3</sub>	<b>71%</b>	<b>331.45 ± 1.167</b>	<b>Good</b>
<b>2b</b>	C <sub>10</sub> H <sub>21</sub>	CH <sub>3</sub>	34%	–	Weak
<b>3b</b>	C <sub>11</sub> H <sub>23</sub>	CH <sub>3</sub>	03%	–	Weak
<b>4b</b>	C <sub>12</sub> H <sub>25</sub>	CH <sub>3</sub>	10%	–	Weak
<b>1c</b>	C <sub>9</sub> H <sub>19</sub>	C <sub>2</sub> H <sub>5</sub>	07%	–	Weak
<b>2c</b>	C <sub>10</sub> H <sub>21</sub>	C <sub>2</sub> H <sub>5</sub>	10%	–	Weak
<b>3c</b>	C <sub>11</sub> H <sub>23</sub>	C <sub>2</sub> H <sub>5</sub>	14%	–	Weak
<b>4c</b>	C <sub>12</sub> H <sub>25</sub>	C <sub>2</sub> H <sub>5</sub>	34%	–	Weak
<b>INDOM<sup>a</sup></b>	–	–	92	273.12 ± 2.33	Standard

Note: Bold values represent significant results.

<sup>a</sup> INDOM: indomethacine (standard drug).

## Conclusions

A series of new *N*-acyl-2-pyrazolines bearing nine to twelve carbon long alkoxy side chains was synthesized to study their solid state self-assembly behavior for understanding the interplay of alkoxy chain crystallization and various supramolecular interactions. Their potential as antifungal and anti-inflammatory agents was also evaluated. Different types of 1D-stacked supramolecular chains are observed for **1b** and **4c** in the crystal lattice, where the difference is only the length of alkoxy chain. These supramolecular structures are stabilized by various CH···O, H···H, CH···π, lonepair···π and π···π interactions. In addition, compounds **2b**, **3b**, **2c** and **3c** show significant to moderate antifungal activity against *Microsporium canis*. However, most of the other compounds are inactive against all the five tested fungal strains. Good anti-inflammatory activity is observed for compound **1b** with IC<sub>50</sub> value 331 μM as compared to 273 μM for standard reference drug. The compounds of the present series as potential chelating agents and with good antifungal and anti-inflammatory properties may be promising future candidates for the design of metal-based therapeutics with higher and improved bioactivities.

## Acknowledgements

The authors A.A. and M.M.N. are grateful to Higher Education Commission (HEC) of Pakistan for financial support. We are also thankful to Panjwani Center for Molecular Medicine and Drug Research, HEJ Research Institute of Chemistry, International Center for Chemical Sciences, University of Karachi, Pakistan for biological studies.

## Appendix A. Supplementary material

Supplementary data associated with this article can be found, in the online version, at <http://dx.doi.org/10.1016/j.saa.2013.10.023>.

## References

- [1] T.M. Acker, A. Khatri, K.M. Vance, C. Slabber, J. Bacska, J.P. Snyder, S.F. Traynelis, D.C. Liotta, J. Med. Chem. 56 (2013) 6434–6456.
- [2] S.P. Sakthinathan, G. Vanangamudi, G. Thirunarayanan, Spectrochim. Acta A 95 (2012) 693–700.

- [3] H.Y. Wang, X.X. Zhang, J.J. Shi, G. Chen, X.P. Xu, S.J. Ji, Spectrochim. Acta A 93 (2012) 343–347.
- [4] S. Ningaiah, U.K. Bhadrachari, S. Keshavamurthy, C. Javarasetty, Bioorg. Med. Chem. Lett. 23 (2013) 4532–4539.
- [5] F.F. Jian, P.S. Zhao, H.M. Guo, Y.F. Li, Spectrochim. Acta A 69 (2008) 647–653.
- [6] P.S. Zhao, R.Q. Li, H.Y. Wang, F.F. Jian, H.M. Guo, Spectrochim. Acta A 74 (2009) 87–93.
- [7] A. Marella, M.R. Ali, M.T. Alam, R. Saha, O. Tanwar, M. Akhter, M. Shaquiquzzaman, M.M. Alam, Mini Rev. Med. Chem. 13 (2013) 921–931.
- [8] S. Kumar, S. Bawa, S. Drabu, R. Kumar, H. Gupta, Recent Pat. Anti-infect. Drug Discov. 4 (2009) 154–163.
- [9] M.R. Shaaban, A.S. Mayhoub, A.M. Farag, Expert Opin. Ther. Pat. 22 (2012) 253–291.
- [10] D. Secci, S. Carradori, A. Bolasco, B. Bizzarri, M.D. Ascenzio, E. Maccioni, Curr. Top. Med. Chem. 12 (2012) 2240–2257.
- [11] K.M. Amin, A.A.M. Eissa, S.M. Abou-Seri, F.M. Awadallah, G.S. Hassan, Euro. J. Med. Chem. 60 (2013) 187–198.
- [12] A. Ciupa, P.A. De Bank, M.F. Mahon, P.J. Wood, Lorenzo Caggiano, Med. Chem. Commun. 4 (2013) 956–961.
- [13] D. Havrylyuk, B. Zimenkovsky, O. Vasylenko, C.W. Day, D.F. Smee, P. Grellier, R. Lesyk, Euro. J. Med. Chem. 66 (2013) 228–237.
- [14] D. Havrylyuk, B. Zimenkovsky, O. Vasylenko, A. Gzella, R. Lesyk, J. Med. Chem. 55 (2012) 8630–8641.
- [15] M.Y. Wani, A.R. Bhat, A. Azam, D.H. Lee, I. Choi, F. Athar, Euro. J. Med. Chem. 54 (2012) 845–854.
- [16] M. Eddaoudi, J. Kim, N. Rosi, D. Vodak, J. Wachter, M. O’Keeffe, O.M. Yaghi, Science 295 (2002) 469.
- [17] X. Li, X. Guo, X. Xu, G. Ma, S. Lin, Inorg. Chem. Commun. 27 (2013) 105.
- [18] F.-K. Wang, S.-Y. Yang, R.-B. Huang, L.-S. Zheng, S.R. Batten, Cryst. Eng. Commun. 10 (2008) 1211.
- [19] C. Janiak, Dalton Trans. (2003) 2781.
- [20] H. Chun, D.N. Dybtsev, H. Kim, K. Kim, Chem. Euro. J. 11 (2005) 3521.
- [21] S. Kitagawa, R. Kitaura, S. Noro, Angew. Chem. Int. Ed. 43 (2004) 2334.
- [22] O.R. Evans, W.B. Lin, Acc. Chem. Res. 35 (2002) 511.
- [23] S.R. Batten, K.S. Murray, Coord. Chem. Rev. 246 (2003) 103.
- [24] M.M. Naseer, S. Hameed, Cryst. Eng. Commun. 14 (2012) 4247.
- [25] L.F. Lindoy, I. Atkinson, Self Assembly in Supramolecular Systems, Monographs in Supramolecular Chemistry, vol. 7, Royal Society of Chemistry, Cambridge, 2000.
- [26] M. Fujita (Ed.), Molecular Self Assembly—Organic Versus Inorganic Approaches, Structure and Bonding, vol. 96, Springer, Berlin, 2000.
- [27] X. Xu, X. Zhang, X. Liu, L. Wang, E. Wang, Cryst. Eng. Commun. 14 (2012) 3264.
- [28] W.L. Leong, J.J. Viital, Chem. Rev. 111 (2011) 688.
- [29] S.R. Batten, N.R. Champness, X.-M. Chen, J.G. Martinez, S. Kitagawa, L. Öhrström, M. O’Keeffe, M.P. Suh, J. Reedijk, Cryst. Eng. Commun. 14 (2012) 3001.
- [30] S.R. Batten, R. Robson, Angew. Chem. Int. Ed. 37 (1998) 1460.
- [31] B. Moulton, M.J. Zaworotko, Curr. Opin. Solid State Mater. Sci. 6 (2002) 117.
- [32] X.T. Wang, Y.L. Bai, F.F. Xing, M. Shao, S.R. Zhu, Inorg. Chem. Commun. 20 (2012) 117.
- [33] R. Dey, B. Bhattacharya, E. Colacio, D. Ghoshal, Dalton Trans. 42 (2013) 2094–2106.
- [34] Y. El Aziz, A.R. Bassindale, P.G. Taylor, R.A. Stephenson, M.B. Hursthouse, R.W. Harrington, W. Clegg, Macromolecules 46 (2013) 988–1001.
- [35] Y.A. Getmanenko, M. Fonari, C. Risko, B. Sandhu, E. Galan, L.Y. Zhu, P. Tongwa, D.K. Hwang, S. Singh, H. Wang, S.P. Tiwari, Y.L. Loo, J.L. Bredas, B. Kippelen, T. Timofeeva, S.R. Marder, J. Mater. Chem. C 1 (2013) 1467–1481.
- [36] A. Lampel, O. Yaniv, O. Berger, E. Bacharach, E. Gazit, F. Frolow, Acta Crystallogr. F 69 (2013) 602–606.
- [37] C.D.P. Klein, G.F. Tabete, A.V. Laguna, U. Holzgrabe, K. Mohr, Euro. J. Pharma. Sci. 14 (2001) 167–175.
- [38] E. Pop, D.C. Oniciu, M.E. Pape, C.T. Cramer, J.-L.H. Dasseux, Croatica Chemica Acta 77 (2004) 301–306.
- [39] A. Hasan, A. Abbas, M.N. Akhtar, Molecules 16 (2011) 7789–7802.
- [40] Stoe & Cie, X-Area Stoe & Cie Darmstadt, Germany, 2001.
- [41] G.M. Sheldrick, SHELXS97 and SHELXL97, University of Göttingen, Germany, 1997.
- [42] A.S. Tan, M.V. Berridge, J. Immunol. Meth. 238 (2000) 59–68.
- [43] E.F. Saad, N.M. Hamada, S.M. Sharaf, S.K. El-Sadany, A.M. Moussa, M. Elba, Rapid Commun. Mass Spectrom. 12 (1998) 833–836.
- [44] C.F. Matta, J. Hernandez-Trujillo, T.H. Tang, R.F. Bader, Chemistry 9 (2003) 1940–1951.
- [45] T.J. Mooibroek, P. Gamez, J. Reedijk, Cryst. Eng. Commun. 10 (2008) 1501–1515.
- [46] A.U. Rahman, M.I. Choudhary, W.J. Thomsen, Bioassay Techniques for Drug Development, Harwood Academic Publishers, The Netherlands, 2001. pp. 22.
- [47] Y. Bellik, L. Boukraâ, H.A. Alzahrani, B.A. Bakhotmah, F. Abdellah, S.M. Hammoudi, M. Iguer-Ouada, Molecules 18 (2013) 322–353.